Cellular/Molecular

The *Drosophila* Receptor Protein Tyrosine Phosphatase LAR Is Required for Development of Circadian Pacemaker Neuron Processes That Support Rhythmic Activity in Constant Darkness But Not during Light/Dark Cycles

Parul Agrawal and Paul E. Hardin
Department of Biology and Center for Biological Clocks Research, Texas A&M University, College Station, Texas 77845-3258

In *Drosophila*, a transcriptional feedback loop that is activated by CLOCK-CYCLE (CLK-CYC) complexes and repressed by PERIOD-TIMELESS (PER-TIM) complexes keeps circadian time. The timing of CLK-CYC activation and PER-TIM repression is regulated post-translationally, in part through rhythmic phosphorylation of CLK, PER, and TIM. Although kinases that control PER, TIM, and CLK levels, activity, and/or subcellular localization have been identified, less is known about phosphatases that control clock protein dephosphorylation. To identify clock-relevant phosphatases, clock-cell-specific RNAi knockdowns of *Drosophila* phosphatases were screened for altered activity rhythms. One phosphatase that was identified, the receptor protein tyrosine phosphatase leukocyte-antigen-related (LAR), abolished activity rhythms in constant darkness (DD) without disrupting the timekeeping mechanism in brain pacemaker neurons. However, expression of the neuropeptide pigment-dispersing factor (PDF), which mediates pacemaker neuron synchrony and output, is eliminated in the dorsal projections from small ventral lateral (sLN_v) pacemaker neurons when *Lar* expression is knocked down during development, but not in adults. Loss of *Lar* function eliminates sLN_v dorsal projections, but PDF expression persists in sLN_v and large ventral lateral neuron cell bodies and their remaining projections. In contrast to the defects in lights-on and lights-off anticipatory activity seen in flies that lack PDF, *Lar* RNAi knockdown flies anticipate the lights-on and lights-off transition normally. Our results demonstrate that *Lar* is required for sLN_v dorsal projection development and suggest that PDF expression in LN_v cell bodies and their remaining projections mediate anticipation of the lights-on and lights-off transitions during a light/dark cycle.

Key words: circadian rhythms; clock genes; locomotor activity; neuropeptides; pacemaker neurons; phosphatase

Significance Statement

In animals, circadian clocks drive daily rhythms in physiology, metabolism, and behavior via transcriptional feedback loops. Because key circadian transcriptional activators and repressors are regulated by phosphorylation, we screened for phosphatases that alter activity rhythms when their expression was reduced. One such phosphatase, leukocyte-antigen-related (LAR), abolishes activity rhythms, but does not disrupt feedback loop function. Rather, *Lar* disrupts clock output by eliminating axonal processes from clock neurons that release pigment-dispersing factor (PDF) neuropeptide into the dorsal brain, but PDF expression persists in their cell bodies and remaining projections. In contrast to flies that lack PDF, flies that lack *Lar* anticipate lights-on and lights-off transitions normally, which suggests that the remaining PDF expression mediates activity during light/dark cycles.

Introduction

A diverse array of animals, plants and microbes display daily rhythms in physiology, metabolism, and/or behavior. These rhythms are not passively driven by environmental cycles, but are controlled by endogenous circadian (~24 h) clocks that keep time in the absence of environmental cues. Circadian clocks in eukaryotes keep time via one or more transcriptional feedback loops that drive daily rhythms in their gene expression. In *Dro-*

Received Dec. 18, 2015; revised Feb. 15, 2016; accepted Feb. 22, 2016.

Author contributions: P.A. and P.E.H. designed research; P.A. performed research; P.A. and P.E.H. analyzed data; P.A. and P.E.H. wrote the paper.

This work was supported by National Institutes of Health Grant NS052854. We thank Michael Rosbash for PER antibody raised in rabbit, Amita Sehgal for TIM antibody raised in rat, Jeff Price for the UAS-*Dicer2*;*tim*Gal4 and *w*;UAS-*Dicer2*;*pdf*Gal4 strains, and Vivek M. Agrawal for his help in writing MATLAB scripts to generate histograms using the ClockLab software.

The authors declare no competing financial interests.

Correspondence should be addressed to Paul E. Hardin, Texas A&M University, 3258 TAMU, BSBW, Room 308a, College Station, TX 77843-3258. E-mail: phardin@bio.tamu.edu.

DOI:10.1523/JNEUROSCI.4523-15.2016

 0270-6474/16/363860-11$15.00/0

Table 1. Activity rhythms are disrupted in clock-cell-specific *Lar* RNAi knockdown and *Lar* mutant flies

Genotype	Total	Rhythmic, %	Period ± SEM	Strength ± SEM
w^{1118};+;+	16	100	23.50 ± 0.00	160.34 ± 21.62
w^{1118};*tim*Gal4/+;+	16	88	23.54 ± 0.04	129.26 ± 11.33
w^{1118};+;*pdf*Gal4/+	16	100	23.66 ± 0.06	118.24 ± 14.20
w^{1118};UAS-*Lar*RNAi/+;+	16	100	23.53 ± 0.03	26.44 ± 9.06
w^{1118};UAS-*Lar*RNAi/*tim*Gal4;+	12	25	24.17 ± 0.27	8.68 ± 1.25*
w^{1118};UAS-*Lar*RNAi/+;*pdf*Gal4/+	16	0	n.a.	2.20 ± 1.03*
UAS-*Dicer2*;*tim*Gal4/+;+	16	100	24.81 ± 0.12	80.85 ± 12.26
UAS-*Dicer2*;UAS-*Lar*RNAi/*tim*Gal4;+	11	0	n.a.	5.00 ± 1.43*
w^{1118};UAS-*Dicer2*/+;*pdf*Gal4/+	15	80	24.17 ± 0.09	62.66 ± 11.51
w^{1118};UAS-*Dicer2*/UAS-*Lar*RNAi; *pdf*Gal4/+	10	10	23.50	5.78 ± 1.22*
w^{1118};*Lar*$^{13.2}$/+;+	14	93	23.54 ± 0.04	59.37 ± 3.23
w^{1118};*Lar* Df/+;+	14	100	23.71 ± 0.11	113.54 ± 29.01
w^{1118};*Lar* Df/*Lar*$^{13.2}$;+	14	0	n.a.	1.83 ± 0.17#

Adult males were entrained in LD for 3 d and transferred to DD for at least 7 d. Analysis of activity rhythms in DD and fly genotypes are as described in Materials and Methods. Total, Number of animals tested; Rhythmic %, percentage of rhythmic animals; Period ± SEM, rhythm period in hours ± SEM; Strength ± SEM, robustness of activity rhythms ± SEM.

*Rhythm strength is significantly different ($p < 0.01$) than w^{1118} and controls containing either the Gal4 driver or UAS responder alone with or without *Dicer2*.

#Rhythm strength is significantly different ($p < 0.001$) than w^{1118}, w^{1118};*Lar* Df/+;+, and w^{1118};*Lar*$^{13.2}$/+;+ flies.

sophila, the core timekeeping loop is initiated by CLOCK-CYCLE (CLK-CYC) heterodimers, which activate *period* (*per*) and *timeless* (*tim*) transcription. Accumulating levels of PER and TIM proteins inhibit CLK-CYC activity, and once PER and TIM are degraded, the next round of CLK-CYC activation can begin (Hardin, 2011). Transcriptional feedback loops driven by orthologous transcriptional regulators function in other animals including humans, indicating that the timekeeping mechanism is highly conserved (Hardin and Panda, 2013; Partch et al., 2014).

The *Drosophila* circadian clock operates in many cells and tissues (Menet and Hardin, 2014). In the brain, this feedback loop operates in ~75 pacemaker neurons per hemisphere that function to drive activity rhythms (Helfrich-Förster, 2003). These brain pacemaker neurons can be divided into multiple clusters based on their location, size and neuropeptide expression, including two anterior dorsal neuron 1 s (DN_{1a}s), ~15 posterior dorsal neuron 1s (DN_{1p}s), two dorsal neuron 2s (DN_2s), ~38 dorsal neuron 3s (DN_3s), six dorsal lateral neurons (LN_ds), three lateral posterior neurons (LPNs), four pigment-dispersing factor (PDF) neuropeptide-expressing small ventral lateral neurons (sLN_vs), one PDF-negative sLN_v, and four large ventral lateral neurons (lLN_vs; Nitabach and Taghert, 2008; Shafer and Yao, 2014). These clusters of pacemaker neurons form a network that maintains synchrony and determines the pattern of activity rhythms based on environmental inputs (Peschel and Helfrich-Förster, 2011; Yoshii et al., 2012). This network also exhibits circadian plasticity; the PDF-positive sLN_vs send axonal projections toward DN_1s and DN_2s that undergo daily changes in morphology (Fernández et al., 2008). However, a direct molecular link between the core clock and rhythmic remodeling of sLN_v axonal projections has not been identified.

The timing of CLK-CYC activation and PER-TIM repression is primarily regulated post-translationally, in part through rhythmic phosphorylation of CLK, PER and TIM to generate ~24 h rhythms. Many kinases have been identified that control PER, TIM, and CLK levels, activity, and/or subcellular localization (Kloss et al., 1998, 2001; Price et al., 1998; Martinek et al., 2001; Lin et al., 2002; Akten et al., 2003, 2009; Chiu et al., 2011; Yu et al., 2011; Szabó et al., 2013). In contrast, few phosphatases have been discovered that target PER, TIM, and/or CLK to regulate transcriptional rhythms (Sathyanarayanan et al., 2004; Fang et al., 2007; Andreazza et al., 2015). To identify additional phosphatases that function within the *Drosophila* circadian clock, we screened for phosphatases that disrupt activity rhythms upon RNAi knockdown in clock cells.

Of 22 phosphatases with aberrant rhythms, the receptor protein tyrosine phosphatase (RPTP) leukocyte-antigen related (LAR; Streuli et al., 1989), is required for rhythmic activity. Despite this behavioral arrhythmicity, clock protein rhythms persist in brain pacemaker neurons from *Lar* mutants and RNAi knockdown flies, which suggest that *Lar* mediates clock output. Indeed, PDF accumulation in sLN_v dorsal projections is eliminated in *Lar* mutant and RNAi knockdown flies, but PDF expression persists in sLN_v cell bodies. The lack of PDF accumulation in sLN_v dorsal projections in *Lar* mutant and RNAi knockdown flies is due to defects in the arborization of these projections during development. Unlike flies deficient in PDF expression or PDF neurons, which lack lights-on anticipation and show premature lights-off anticipation (Renn et al., 1999), *Lar* RNAi knockdown flies show normal lights-on and lights-off anticipation. Because PDF expression in sLN_v and lLN_v cell bodies and their surviving projections distinguish *Lar* mutants and RNAi knockdown flies from flies lacking PDF entirely, our results suggest that the remaining PDF expression in sLN_v and lLN_vs mediate lights-on and lights-off anticipation during light/dark cycles.

Materials and Methods

Fly strains. The following *Drosophila* strains were used in this study: w^{1118}, w^{1118};Cyo/Sco;TM2/TM6B, w^{1118};*tim*Gal4, w^{1118};;*pdf*Gal4, *w;; tim*Gal4, UAS-*Lar*RNAi (P{KK100581}, VDRC), UAS-*Lar* (*w*;P{UAS-*Lar*.K}P4B, BDSC), UAS-*Dicer2*;*tim*Gal4, and *w*;UAS-*Dicer2*;*pdf*Gal4 (gifts from Jeffery Price, University of Missouri, Kansas City MO), UAS-mCD8::GFP (*w*;P{UAS-mCD8::GFP.L}LL6, BDSC), *tub*Gal80^{ts} (P{tubP-Gal80^{ts}}20, BDSC), *Lar*$^{13.2}$ (*w*;*Lar*$^{13.2}$/CyO, BDSC), *Lar* Df (Df(2L)E55, *rdo*^{1} *hook*^{1} *Lar*^{E55} *pr*^{1}/CyO, BDSC), and *y w*;;*pdf*^{01} (a gift from Paul Taghert Washington University, St. Louis, MO). Flies were reared on standard cornmeal/agar medium supplemented with yeast and kept in 12 h light/12 h dark (LD) cycles at 25°C. The *Lar* mutant strains, *Lar*$^{13.2}$ and *Lar* Df were backcrossed seven times to *y*^{1};P{SUPor-P}*Lar*^{KG04810}/CyO;*ry*^{506} flies (BDSC) to minimize effects due to differences in genetic background.

Drosophila activity monitoring and behavior analysis. One- to 3-d-old male flies were entrained for 3 d in LD cycles and transferred to constant darkness (DD) for 7 d at 25°C. To knockdown *Lar* only in adults using the TARGET system (McGuire et al., 2003), w^{1118};UAS-*Lar*RNAi/*tub*Gal80^{ts};*pdf*Gal4/+ males were raised at the permissive temperature (18°C) for *tub*Gal80^{ts} to block Gal4-dependent expression of *Lar* RNAi. After eclosion, flies were entrained for 3 d in LD and monitored for 7 d in DD at the restrictive temperature (30°C), which allows Gal4-dependent expression of *Lar* RNAi. Controls lacking *Lar* expression in adults and during development were raised and tested at 18°C. To express *Lar* RNAi only during development, w^{1118};UAS-*Lar*RNAi/*tub*Gal80^{ts};*pdf*Gal4/+ males were raised at 30°C to allow Gal4-dependent *Lar* RNAi expression. After eclosion, flies were entrained for 3 d in LD and monitored for 7 d in DD at the permissive temperature (18°C). Controls that express *Lar* during development and in adults were raised and tested at 30°C. Locomotor activity was monitored using the *Drosophila* Activity Monitor system (Trikinetics). To determine period and rhythm strength during DD, χ^2 periodogram analysis was performed using ClockLab (Actimetrics) software as previously described (Pfeiffenberger et al., 2010). Flies were considered rhythmic if their χ^2 power value was ≥10 above the significance line (ie, strength ≥10) and they were clearly rhythmic by visual inspection of the actogram. For analysis of activity during LD conditions, flies were monitored for 7 d. The number of activity events were recorded in 30 min bins, and average numbers of activity events per 30 min bin per fly

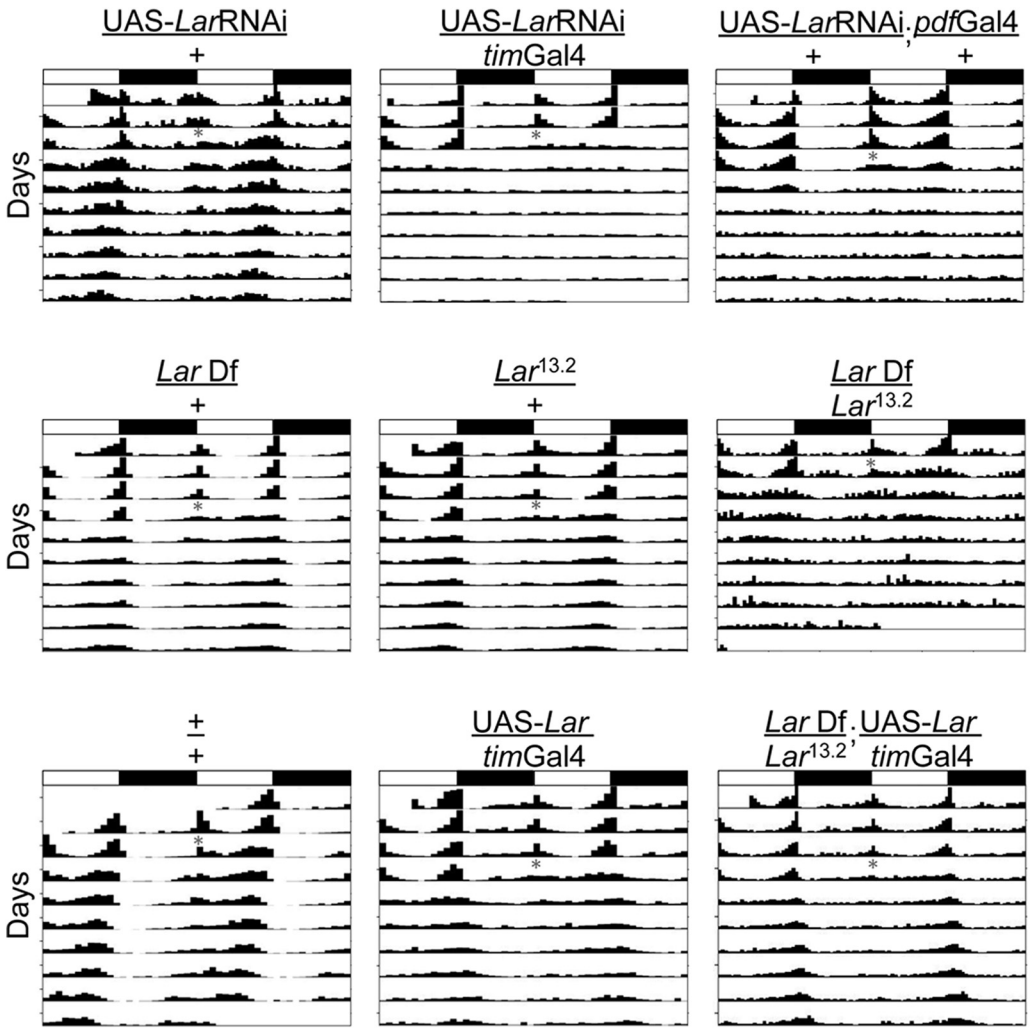

Figure 1. Locomotor activity analysis of clock-cell-specific *Lar* RNAi knockdown and *Lar* mutant flies. Adult males of the indicated genotypes were entrained in LD for 3 d and transferred to DD (gray asterisk) for at least 7 d. Analysis of activity in DD and fly genotypes are as described in Materials and Methods. Representative double-plotted actograms for single flies of each genotype are shown. White boxes, lights-on period; black boxes, lights-off period; vertical bars, fly activity. The height of vertical bars indicates relative level of activity.

Table 2. *Lar* expression in clock cells rescues activity rhythms in *Lar* mutant and RNAi knockdown flies

Genotype	Total	Rhythmic, %	Period ± SEM	Strength ± SEM
w^{1118};+;UAS-*Lar*/+	14	100	23.57 ± 0.04	92.86 ± 9.91
w^{1118};+;*tim*Gal4/+	15	93	23.58 ± 0.06	58.54 ± 4.63
w^{1118};+;UAS-*Lar*/*tim*Gal4	16	88	24.20 ± 0.32	65.16 ± 5.98†
w^{1118};*Lar* Df/*Lar* $^{13.2}$;UAS-*Lar*/*tim*Gal4	14	86	24.67 ± 0.10	26.70 ± 7.05*
w^{1118};UAS-*Dicer2*/+;UAS-*Lar*/*tim*Gal4	15	80	24.21 ± 0.22	29.95 ± 8.61
w^{1118};UAS-*Dicer2*/UAS-*Lar*RNAi; UAS-*Lar*/*tim*Gal4	16	88	24.54 ± 0.24	14.61 ± 1.14#

Adult flies were entrained in LD for 3 d and transferred to DD for at least 7 d. Analysis of activity rhythms in DD and fly genotypes are as described in Materials and Methods. The Total, Rhythmic %, Period ± SEM, and Power ± SEM columns are as described in Table 1.

*Rhythm strength is significantly different ($p < 0.004$) than w^{1118};*Lar* $^{13.2}$/+;+ and w^{1118};*Lar* Df/+;+ flies (Table 1).

#Rhythm strength is significantly different ($p = 0.02$) than UAS-*Dicer2*;UAS-*Lar*RNAi/*tim*Gal4;+flies (Table 1).

†Rhythm strength is significantly different ($p = 0.011$) than w^{1118};+;UAS-*Lar*/+, but not significantly different ($p = 0.39$) than w^{1118};+;*tim*Gal4/+.

were calculated to generate histograms. The times of morning and evening activity peaks (phase values) were computed using ClockLab. Morning Anticipation Index values were calculated as the ratio of activity counts occurring 3 h before lights-on over activity counts occurring 6 h before lights-on as described previously (Harrisingh et al., 2007; De et al., 2013). All *p* values were calculated using a Student's two-tailed *t* test with unequal variance.

Immunohistochemistry. Antibody staining of larval CNSs and adult fly brains was performed as previously described (Houl et al., 2008). Briefly, larval CNSs and adult brains were dissected in 1× PBS and fixed with 3.7% formaldehyde in 1× PBS at room temperature (RT) for 15 min. Samples were then washed and incubated with blocking solution containing 1× PBS, 5% BSA, 5% goat serum (5% donkey serum for primary antibodies raised in goat), 0.03% sodium deoxycholate, and 0.03% TritonX100 at RT for 1 h followed by incubation with primary antibodies overnight (ON) at 4°C in blocking solution. Primary antibodies and their dilutions used were as follows: guinea pig anti-CLK GP50 1:3000 (Houl et al., 2008), goat anti-CLK dC-17 (Santa Cruz Biotechnology) 1:100, rabbit anti-GFP ab6556 (Abcam) 1:500, pre-absorbed rabbit anti-PER (gift from Michael Rosbash, Brandeis University, Waltham, MA) 1:15,000, and mouse anti-PDF (Developmental Studies Hybridoma Bank) 1:500. For detection of primary antisera, the following secondary antibodies were used at a dilution of 1:200 (incubated ON at 4°C) in blocking solution: goat anti-rabbit AlexaFluor 488 (Invitrogen), donkey anti-rabbit AlexaFluor 647 (Invitrogen), goat anti-guinea pig Cy-3 (Jackson ImmunoResearch Laboratories), donkey anti-guinea pig AlexaFluor 488 (Invitrogen), goat anti-mouse AlexaFluor 488 and AlexaFluor 647 (Invitrogen), and donkey anti-goat AlexaFluor 488 (Invitrogen). Brains were then mounted in Vectashield mounting medium (Vector Labora-

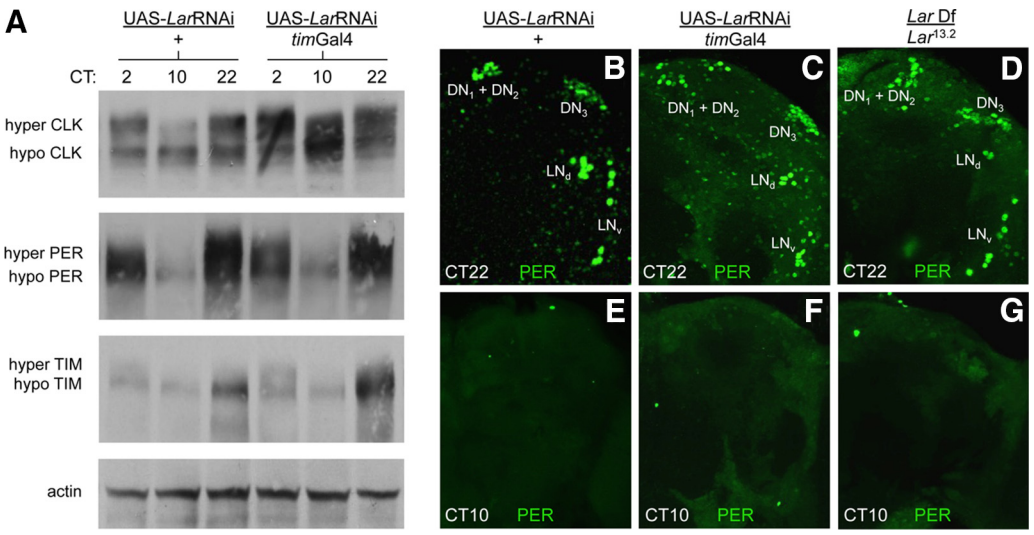

Figure 2. Rhythms in clock gene expression are intact in *Lar* knockdown flies. Flies were entrained for 3 d in LD conditions and collected at the indicated times on the first day of DD for Western analysis or the third day of DD for PER immunostaining. ***A***, Western blots of head extracts from w^{1118};UAS-*Lar*RNAi/+ and UAS-*Dicer2*/+;UAS-*Lar*RNAi/*tim*Gal4 (UAS-*Lar*RNAi/*tim*Gal4) flies were probed with CLK, PER, and TIM antisera. Bands corresponding to hyperphosphorylated CLK, PER, and TIM (hyperCLK, hyperPER, and hyperTIM, respectively) and hypophosphorylated CLK, PER, and TIM (hypoCLK, hypoPER, hypoTIM, respectively) are shown. Actin serves as a loading control. ***B***–***G***, Brains dissected from adult flies collected at CT22 or CT10 were immunostained with PER antisera and imaged by confocal microscopy. ***B***, ***E***, Projected *Z*-series images of right brain hemispheres from w^{1118};UAS-*Lar*RNAi/+ flies. ***C***, ***F***, Projected *Z*-series images of right brain hemispheres from UAS-*Dicer2*/+;UAS-*Lar*RNAi/*tim*Gal4 (UAS-*Lar*RNAi/*tim*Gal4) flies. ***D***, ***G***, Projected *Z*-series images of right brain hemispheres from Df(2L)E55/$Lar^{13.2}$ (*Lar* Df/$Lar^{13.2}$) flies. PER staining is detected in all three groups of dorsal neurons (DN_1+DN_2, DN_3); LN_d; and LN_v. All images are representative of nine or more fly brains.

tories) for imaging. Entrained L3 larvae or 1- to 5-d-old adults were used for dissection.

Imaging. Larval CNSs and adult fly brains were imaged using an Olympus FV1000 confocal microscope (Olympus America) as described previously (Liu et al., 2015). Briefly, serial optical scans were obtained at 2 μm intervals without using Kalman-averaging. For coimmunostaining experiments, sequential scans of the Argon 488 nm and HeNe (543 nm for Cy3, 633 nm for AlexaFluor 647 and Cy5) lasers were used to avoid bleed-through between channels. For imaging AlexaFluor 488 and Cy3; Argon 488 nm and HeNe 543 nm lasers were used, with the 405/488/543 nm dichronic mirror for excitation whereas for imaging AlexaFluor 488 and either AlexaFluor 647 or Cy5; Argon 488 nm and HeNe 633 nm lasers were used, with the 488/543/633 nm dichronic mirror for excitation. Fluorescence signals were separated by a beam splitter (560-nm-long pass) and recorded on spectral detectors set to 500–530 nm for AlexaFluor 488, 555–655 nm for Cy3, and a detector with 650-nm-long pass filter for AlexaFluor 647 or Cy5. The Fluoview "Hi-Lo" lookup table was used to set the maximal signal below saturation and set the background to near zero using the high voltage and offset controls. Original Olympus images were saved as 12 bit oib format and processed using FV1000 confocal software to generate Z-stack series. Images were adjusted for brightness and contrast using FV1000 confocal software when needed. For each genotype and developmental stage, brain images were acquired using the same settings (power, gain, offset) at the same time.

Western blot analysis. For preparing protein extract from adult fly heads, flies were entrained in LD cycles for at least 3 d and collected at circadian time (CT)2, CT10, and CT22 on day 1 of constant darkness. Lysis was performed in radioimmunoprecipitation assay buffer (20 mM Tris, pH 7.5, 150 mM NaCl, 1 mM EDTA, 0.05 mM EGTA, 10% glycerol, 1% Triton X-100, 0.4% sodium deoxycholate, 0.1% SDS) containing protease inhibitor mixture (0.5 mM phenylmethylsulfonyl fluoride, 10 μg/ml aprotinin, 10 μg/ml leupeptin, 2 μg/ml pepstatin A, 1 mM Na_3VO_4, and 1 mM NaF). This homogenate was sonicated five to eight times for 10 s each, using a Microson ultrasonic cell disruptor at a setting of 4–5, and then centrifuged at 20,000 $\times$ *g* for 10 min. The supernatant was collected and protein concentration was determined by the Coomassie-based Bradford Assay. Three hundred nanograms of total protein for each genotype were loaded in each lane. Soluble protein extracts were separated on 5% polyacrylamide electrophoresis gels, transferred to supported nitrocellulose membranes (MSI) and incubated with GP50 anti-CLK (1:4000), pre-absorbed rabbit anti-PER (1:65,000, gift from Michael Rosbash), rat anti-TIM (1:1000, gift from Amita Sehgal, University of Pennsylvania, Philadelphia, PA), or anti-β-ACTIN (1:5000; Sigma-Aldrich) antibodies. Goat anti-rabbit, anti-guinea-pig, anti-rat, and anti-mouse conjugated to horseradish peroxidase were used at a 1:2000 dilution (Jackson Immunoresearch) as secondary antibodies. Chemiluminescent detection was used to develop the reaction using ECL plus (GE Healthcare) reagent.

Results

Reducing LAR expression in clock cells abolishes activity rhythms

In *Drosophila*, release of transcriptional repression by the degradation of PER and TIM proteins occurs simultaneously with the replacement of hyperphosphorylated CLK by transcriptionally competent hypophosphorylated CLK (Yu et al., 2006). Likewise, multiple kinases and phosphatases control the phosphorylation state of PER and TIM, which determines the timing of transcriptional repression by regulating their nuclear localization and stability (Hardin, 2011). We sought to identify phosphatases that promote CLK-CYC transcriptional activation upon dephosphorylation of core clock components. The loss of such phosphatases is predicted to delay CLK-CYC transcriptional activity, slow PER-TIM degradation, and/or their nuclear localization; all of which act to lengthen circadian period (Sathyanarayanan et al., 2004; Fang et al., 2007; Andreazza et al., 2015).

To identify phosphatases that dephosphorylate clock proteins, we used clock-cell-specific RNAi knockdown to screen a total of ~100 protein phosphatases for altered locomotor activity rhythms. The *tim*Gal4 and *pdf*Gal4 drivers were used to express UAS-phosphatase RNAi in either all clock cells or in PDF-positive LN_vs alone. The screen identified 22 genes that either lengthened or shortened circadian period by $\geq$1 h ($p \leq 0.05$ compared with controls) or were arrhythmic. An RNAi line targeting the RPTP *Lar* (UAS-*Lar*RNAi) was largely arrhythmic when driven by either *tim*Gal4 or *pdf*Gal4 during DD, whereas *tim*Gal4, *pdf*Gal4 and UAS-*Lar*RNAi controls showed high levels

of rhythmicity (Table 1; Fig. 1). When UAS-*Dicer2* was used to enhance the RNAi potency (Dietzl et al., 2007), flies expressing *Lar* RNAi in all clock cells or PDF-positive LN_vs were almost entirely arrhythmic (Table 1). Whether or not *Dicer2* was used to enhance *Lar* RNAi potency, knocking down *Lar* expression in clock cells caused a significant ($p < 0.01$) increase in arrhythmicity.

To independently confirm that decreased *Lar* expression abolishes activity rhythms, we tested loss of function *Lar* mutants for behavioral defects. *Lar*-null mutants, although capable of completing embryogenesis and early larval development, die as late third instar larvae or pupae (Krueger et al., 1996). Because homozygous *Lar*-null mutants do not survive to adulthood, we tested transheterozygous combinations of isogenized *Lar* loss-of-function alleles for locomotor activity rhythms. One allelic combination, *Lar* deficiency Df(2L)E55 over point mutant $Lar^{13.2}$ (*Lar* Df/$Lar^{13.2}$), was viable, even though both alleles are predicted to be null for LAR function (Krueger et al., 1996). Activity rhythms in *Lar* Df/$Lar^{13.2}$ flies were abolished, as reflected by a significant ($p < 0.001$) decrease in rhythm strength compared with *Lar* Df/+ and $Lar^{13.2}$/+ flies (Table 1; Fig. 1), thus confirming the behavioral phenotype and the specificity of *Lar* RNAi.

Because reduced levels of *Lar* in clock-cell-specific *Lar* RNAi knockdown and *Lar* Df/$Lar^{13.2}$ flies caused high levels of arrhythmicity, we reasoned that expressing *Lar* specifically in clock cells would rescue the arrhythmic phenotype associated with these genotypes. To express *Lar* in clock cells, *tim*Gal4 was used to drive UAS-*Lar*. When *tim*Gal4 was used to express UAS-*Lar* in clock-cell-specific *Lar* RNAi knockdown or *Lar* Df/$Lar^{13.2}$ mutant flies, rhythmic activity was restored (Table 2; Fig. 1), consistent with the significant increase in rhythm strength compared with control *tim*Gal4 driven *Lar* RNAi ($p = 0.0032$) and *Lar* Df/$Lar^{13.2}$ ($p = 0.02$) flies (Table 1). Rescue of clock-cell-specific *Lar* RNAi knockdown and *Lar* Df/$Lar^{13.2}$ arrhythmicity by clock-cell-specific *Lar* expression further demonstrates that LAR levels and/or activity are required for rhythmic activity.

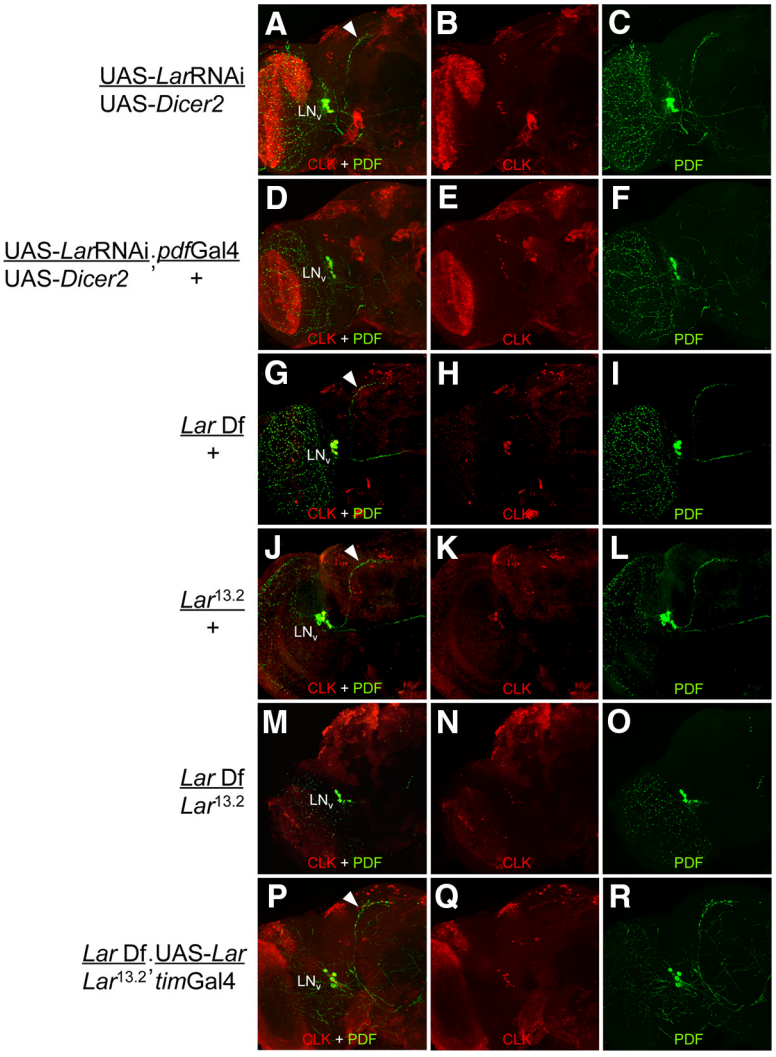

Figure 3. PDF expression is absent in sLN_v dorsal projections of PDF neuron-specific *Lar* RNAi knockdown flies. Brains dissected from adult flies collected at ZT2 were immunostained with CLK and PDF antibodies and imaged by confocal microscopy. Each image shows a left brain hemisphere, where lateral is right and dorsal is at the top. ***A–C***, Projected *Z*-series image (76 μm) of a UAS-*Lar*RNAi/UAS-*Dicer2* brain. ***D–F***, Projected *Z*-series image (90 μm) of a UAS-*Lar*RNAi/UAS-*Dicer2*;*pdf*-Gal4/+ brain. ***G–I***, Projected *Z*-series image (76 μm) of a *Lar* Df/+ brain. ***J–L***, Projected *Z*-series image (78 μm) of a $Lar^{13.2}$/+ brain. ***M–O***, Projected *Z*-series image (88 μm) of a *Lar* Df/$Lar^{13.2}$ brain. ***P–R***, Projected *Z*-series image (82 μm) of a *Lar* Df/$Lar^{13.2}$;*tim*Gal4/UAS-*Lar* brain. Colocalization of PDF (green) and CLK (red) is seen as yellow. LN_v denotes the position of LN_v cell bodies. White arrowhead denotes the sLN_v dorsal projection. All images are representative of nine or more fly brains.

Molecular clock gene oscillations are preserved in *Lar* knockdown flies

Because *Lar* is an RPTP, we expected that reducing LAR levels would result in increased clock protein phosphorylation, thus disrupting feedback loop progression and/or function. To determine whether reducing *Lar* expression alters PER, TIM and/or CLK phosphorylation or abundance, antibodies against these proteins were used to probe Western blots containing head extracts from *tim*Gal4 driven UAS-*Lar*RNAi and UAS-*Lar*RNAi flies without a Gal4 driver collected at different Zeitgeber times (ZTs; where ZT0 is lights-on and ZT12 is lights-off) during LD cycles or different CTs (where CT0 is subjective lights-on and CT12 is subjective lights-off) during DD. CT2, CT10, and CT22 time points were selected to detect differences in abundance and/or phosphorylation because higher levels and/or hyperphosphorylated forms of clock proteins are present at CT22 and CT2 and lower levels and/or hypophosphorylated forms of clock proteins are present at CT10. Neither CLK, PER, and TIM phosphorylation, as measured by the lower mobility forms, nor abundance were noticeably different in head extracts from *tim*Gal4 driven UAS-*Lar*RNAi and control UAS-*Lar*RNAi/+ flies during LD (data not shown) or DD conditions (Fig. 2*A*). This result demonstrates that the molecular oscillator in clock-cell-specific *Lar* RNAi knockdown flies is functioning similar to that in controls having normal *Lar* levels, at least in fly heads, where >90% clock protein signal comes from photoreceptor expression (Glossop and Hardin, 2002).

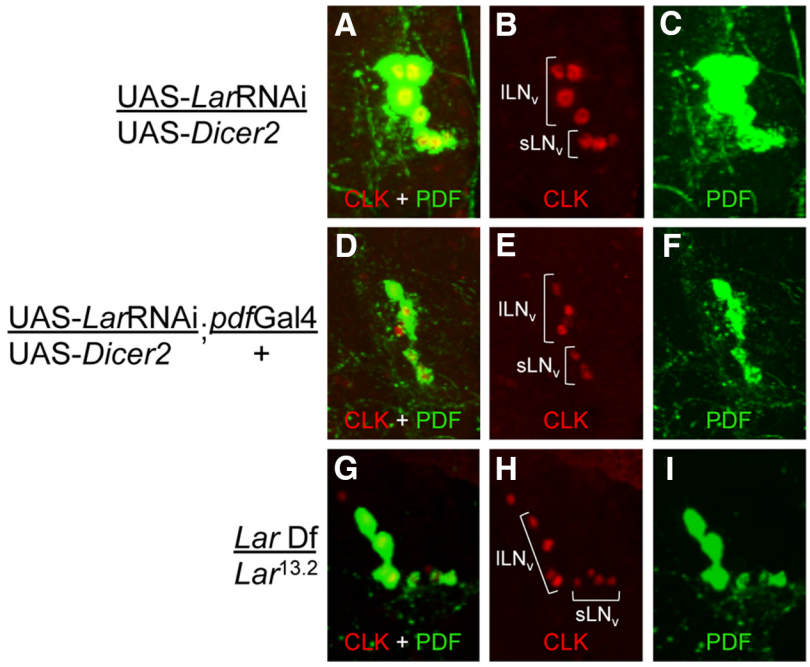

Figure 4. Both lLN$_v$s and sLN$_v$s are present in PDF neuron-specific *Lar* RNAi knock down and *Lar* Df/*Lar*$^{13.2}$ mutant flies. Brains dissected from adult flies collected at ZT2 were immunostained with CLK and PDF antibodies and the region containing LN$_v$s was imaged by confocal microscopy. ***A–C***, Projected *Z*-series (18 μm) from a UAS-*Lar*RNAi/UAS-*Dicer2* brain. ***D–F***, Twelve micrometer projected *Z*-series image from a UAS-*Lar*RNAi/UAS-*Dicer2*;*pdf*Gal4/+ brain. ***G–I***, Fourteen micrometer projected *Z*-series image from a *Lar* Df/*Lar*$^{13.2}$ brain. Colocalization of PDF (green) and CLK (red) is seen as yellow. All images are representative of eight or more fly brains.

To directly assess clock protein localization and cycling in pacemaker neurons in clock-cell-specific *Lar* RNAi knockdown and *Lar* Df/*Lar*$^{13.2}$ flies, PER distribution was monitored in dissected brains during LD (data not shown) and DD. Newly eclosed UAS-*Lar*RNAi/+, *tim*Gal4 driven UAS-*Lar*RNAi and *Lar* Df/*Lar*$^{13.2}$ adults were synchronized in LD and collected for dissection at the predicted PER peak (CT22) and trough (CT10) time points on the third day after transfer to DD. Remarkably, PER expression in *tim*Gal4 driven UAS-*Lar*RNAi and *Lar* Df/*Lar*$^{13.2}$ brains was indistinguishable from UAS-*Lar*RNAi/+ controls at both peak and trough time points during LD (data not shown) and DD (Fig. 2*B–G*). In each of these genotypes, PER was readily detected in all pacemaker neuron groups at CT22 (Fig. 2*B–D*), but was undetectable at CT10 (Fig. 2*E–G*). Cycling of PER protein in whole heads from *tim*Gal4 driven UAS-*Lar*RNAi flies and pacemaker neurons from *tim*Gal4 driven UAS-*Lar*RNAi and *Lar* Df/*Lar*$^{13.2}$ flies demonstrates that *Lar* does not disrupt molecular oscillator function. These results suggest that *Lar* functions downstream of the molecular oscillator to disrupt activity rhythms.

PDF accumulation is impaired in *Lar* knockdown flies

A key regulator of locomotor activity rhythms is the neuropeptide PDF (Renn et al., 1999), which rhythmically accumulates in the sLN$_v$ projections into the dorsal brain (hereafter sLN$_v$ dorsal projections) with a peak early in the day (Park et al., 2000). To determine whether defects in PDF expression give rise to the arrhythmic activity seen in clock-cell-specific *Lar* RNAi knockdown and *Lar* Df/*Lar*$^{13.2}$ mutant flies, PDF was monitored in brains from PDF neuron-specific *Lar* RNAi knockdown, *Lar* Df/*Lar*$^{13.2}$ mutant and control flies at ZT2. In *pdf*Gal4 driven UAS-*Lar*RNAi flies, PDF immunostaining is markedly reduced or absent (18 of 18 brain hemispheres) in sLN$_v$ dorsal projections compared with the normal PDF immunostaining (18 of 18 brain hemispheres) seen in sLN$_v$ dorsal projections from control UAS-*Lar*RNAi flies (Fig. 3*A–F*). In contrast, PDF immunostaining in lLN$_v$ projections to the medulla and accessory medulla (aMe) showed no alterations in *pdf*Gal4 driven UAS-*Lar*RNAi or control UAS-*Lar*RNAi flies (18 of 18 brain hemispheres for each genotype; Fig. 3*A–F*), whereas PDF immunstaining in lLN$_v$ projections to the posterior optic tract (POT) were absent or disrupted in most *pdf*Gal4 driven UAS-*Lar*RNAi flies (10 of 18 brain hemispheres) but normal in UAS-*Lar*RNAi controls (18 of 18 brain hemispheres) (Fig. 3*A–F*). Likewise, wild-type PDF immunostaining was detected in sLN$_v$ dorsal projections from *Lar* Df/+ and *Lar*$^{13.2}$/+ control flies (16 of 16 brain hemispheres for each genotype), but PDF immunostaining was absent in sLN$_v$ dorsal projections in *Lar* Df/*Lar*$^{13.2}$ mutants (16 of 16 brain hemispheres; Fig. 3*G–O*). PDF expression in lLN$_v$ projections to the medulla and aMe were present but appeared less intense in *Lar* Df/*Lar*$^{13.2}$ mutants than in control *Lar* Df/+ and *Lar*$^{13.2}$/+ flies (16 of 16 brain hemispheres), and PDF levels in the POT projection were drastically reduced or absent in *Lar* Df/*Lar*$^{13.2}$ mutant flies (8 of 16 brain hemispheres) compared with *Lar* Df/+ and *Lar*$^{13.2}$/+ controls (Fig. 3*G–O*).

If the lack of PDF accumulation in sLN$_v$ dorsal projections is due to decreased *Lar* levels, then expressing *Lar* in clock cells should restore PDF expression in these projections. Indeed, when *tim*Gal4 was used to drive UAS-*Lar* in *Lar* Df/*Lar*$^{13.2}$ flies, wild-type PDF immunostaining was detected in sLN$_v$ dorsal projections and lLN$_v$ medulla projections (16 of 16 brain hemispheres; Fig. 3*P–R*). However, PDF expression in lLN$_v$ POT projections was not completely restored by expressing *Lar* in all clock neurons (8 of 16 brain hemispheres were disrupted or absent; Fig. 3*P–R*). The lack of PDF accumulation in sLN$_v$ dorsal projections is not due to the loss of sLN$_v$s in flies with impaired *Lar* expression; CLK is expressed in sLN$_v$ nuclei of *pdf*Gal4 driven UAS-*Lar*RNAi flies, *Lar* Df/*Lar*$^{13.2}$ mutants and control flies with varying levels of PDF (Fig. 4). CLK levels in *pdf*Gal4 driven UAS-*Lar*RNAi and *Lar* Df/*Lar*$^{13.2}$ mutant flies were not significantly different ($p > 0.05$) than the UAS-*Lar*RNAi and *Lar* Df/+ or *Lar*$^{13.2}$/+ controls, respectively. These data demonstrate that LAR expression in PDF neurons is required for PDF accumulation in sLN$_v$ dorsal projections.

Lar is required during development for PDF accumulation in sLN$_v$ dorsal projections and activity rhythms

Loss of *Lar* expression in pacemaker neurons could abolish activity rhythms and PDF accumulation in sLN$_v$ dorsal projections by blocking clock output pathway development, maintenance, or both. To determine whether LAR is required in adults for locomotor activity rhythms, *Lar* RNAi was expressed in PDF-expressing neurons post-eclosion using the Gal80^{ts} TARGET system (McGuire et al., 2003). In flies raised and tested at the permissive temperature (18°C), Gal80^{ts} inhibits *pdf*Gal4 driven UAS-*Lar*RNAi, resulting in rhythms with a period of 23.54 h

Table 3. PDF neuron-specific *Lar* RNAi knockdown during development, but not in adults, abolishes activity rhythms

Genotype (temperature raised ≫ temperature tested)	Total	Rhythmic, %	Period ± SEM	Strength ± SEM
w^{1118};+;+ (18°C ≫ 30°C)	16	94	23.50 ± 0.12	29.35 ± 12.45
w^{1118};*tub*-Gal80^{ts}/+;*pdf*Gal4/+ (18°C ≫ 30°C)	18	89	23.94 ± 0.13	14.05 ± 2.55
w^{1118};UAS-*Lar*RNAi/+;+ (18°C ≫ 30°C)	15	100	23.59 ± 0.08	21.41 ± 4.46
w^{1118};UAS-*Lar*RNAi/*tub*-Gal80^{ts};*pdf*Gal4/+ (18°C ≫ 30°C)	18	94	23.46 ± 0.21	17.62 ± 3.05
w^{1118};+;+ (30°C ≫ 30°C)	12	92	24.41 ± 0.11	17.48 ± 2.01
w^{1118};*tub*-Gal80^{ts}/+;*pdf*Gal4/+ (30°C ≫ 30°C)	15	87	24.04 ± 0.13	31.75 ± 10.01
w^{1118};UAS-*Lar*RNAi/+;+ (30°C ≫ 30°C)	14	93	23.61 ± 0.14	16.21 ± 1.8
w^{1118};UAS-*Lar*RNAi/*tub*-Gal80^{ts};*pdf*Gal4/+ (30°C ≫ 30°C)	18	6	24.50	3.44 ± 1.17*
w^{1118};+;+ (18°C ≫ 18°C)	12	83	23.45 ± 0.05	35.13 ± 9.46
w^{1118};*tub*-Gal80^{ts}/+;*pdf*Gal4/+ (18°C ≫ 18°C)	12	83	23.30 ± 0.08	43.76 ± 7.94
w^{1118};UAS-*Lar*RNAi/+;+ (18°C ≫ 18°C)	16	88	23.50 ± 0.10	15.01 ± 1.34
w^{1118};UAS-*Lar*RNAi/*tub*-Gal80^{ts};*pdf*Gal4/+ (18°C ≫ 18°C)	17	88	23.61 ± 0.09	47.37 ± 6.31
w^{1118};+;+ (30°C ≫ 18°C)	12	92	23.43 ± 0.03	27.79 ± 6.23
w^{1118};*tub*-Gal80^{ts}/+;*pdf*Gal4/+ (30°C ≫ 18°C)	15	80	23.71 ± 0.16	30.67 ± 18.72
w^{1118};UAS-*Lar*RNAi/+;+ (30°C ≫ 18°C)	12	83	23.56 ± 0.07	13.48 ± 2.06
w^{1118};UAS-*Lar*RNAi/*tub*-Gal80^{ts};*pdf*Gal4/+ (30°C ≫ 18°C)	15	13	24.75 ± 0.11	6.85 ± 1.47*

Adult males of the indicated genotypes were either raised (first temperature in parenthesis) at the permissive temperature (18°C) to block Gal4-dependent expression of *Lar* RNAi or the restrictive temperature (30°C) to permit Gal4-dependent expression of *Lar* RNAi. After eclosion, adult flies of the indicated genotype were entrained for 3 d in LD and monitored for seven days in constant darkness (second temperature in parenthesis) at either 18°C or 30°C. Flies raised and/or tested at 30°C showed a 30–50% lower survival rate. Analysis of activity in DD and fly genotypes are as described in Materials and Methods. The Total, Rhythmic %, Period ± SEM, and Power ± SEM columns are as described in Table 1.

*Significantly different ($p < 0.05$) rhythm strength compared to controls exposed to the same temperature regime. *Lar* RNAi knockdown flies raised at 18°C and tested at 30°C were not significantly different ($p > 0.29$) than controls exposed to this temperature regime. *Lar* RNAi knockdown flies raised and tested at 18°C were not significantly different ($p > 0.28$) than all controls exposed to this temperature regime except for UAS-*Lar* RNAi flies, which had significantly ($p < 0.01$) weaker rhythms.

(Table 3, row 12), and strengths that were either not different ($p > 0.28$) or stronger ($p < 0.02$) than controls unable to express *Lar* RNAi (Table 3, rows 9–11). When *pdf*-Gal4 driven UAS-*Lar*RNAi flies were raised at 18°C and transferred to restrictive temperature (30°C) after eclosion, *Lar* RNAi is only expressed in PDF neurons of adults. However, these flies were just as rhythmic ($p > 0.29$) as control flies that are unable to express *Lar* RNAi after eclosion and had comparable periods (Table 3, compare row 4 to rows 1–3). These results suggest that LAR expression in PDF neurons after adults emerge is not required for activity rhythms. This result implies that *Lar* function is required in sLN$_v$s during development since knocking down *Lar* in PDF neurons during development and in adults essentially eliminates activity rhythms (Table 1, rows 6 and 10).

To confirm a role for LAR during development, we tested *pdf*Gal4 driven UAS-*Lar*RNAi flies for defects in activity rhythms when raised and tested at 30°C at the adult stage (continuous *Lar* knockdown) or raised at 30°C and transferred to 18°C at the adult stage (development only *Lar* knockdown). Both continuous and development-only *Lar* knockdown flies displayed significantly higher arrhythmicity ($p < 0.05$) compared with control strains that showed rhythms with 23.5–24.5 h circadian periods (Table 3, compare row 8 to rows 5–7 and row 16 to rows 13–15). These results confirm that *Lar* is required during early stages of fly development for rhythms in locomotor activity.

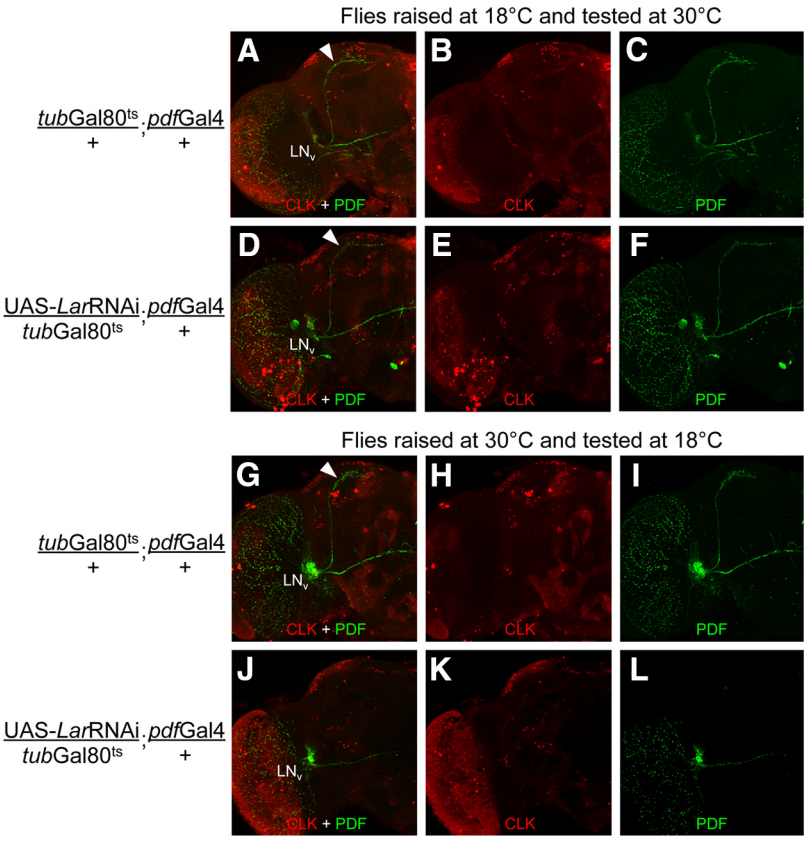

Figure 5. *Lar* is required during development, but not in adults, for PDF accumulation in sLN$_v$ dorsal projections. ***A–F***, Flies were raised at 18°C to block Gal4 activation, shifted to 30°C after eclosion to permit Gal4 activation, and collected at ZT2. ***A–C***, Seventy-four micrometer projected *Z*-series image of a *tub*Gal80^{ts}/+;*pdf*Gal4/+ brain. ***D–F***, Eighty-two micrometer projected *Z*-series image of a UAS-*Lar*RNAi/*tub*Gal80^{ts};*pdf*Gal4/+ brain. ***G–L***, Flies were raised at 30°C to permit Gal4 activation, shifted to 18°C after eclosion to block Gal4 activation, and collected at ZT2. ***G–I***, Eighty-six projected *Z*-series image of a *tub*Gal80^{ts}/+;*pdf*Gal4/+ brain. ***J–L***, Eighty-two micrometer projected *Z*-series image of a UAS-*Lar*RNAi/*tub*Gal80^{ts};*pdf*Gal4/+ brain. Brains were dissected, immunostained with CLK and PDF antibodies, and imaged by confocal microscopy. A left brain hemisphere is shown in each image, where lateral is right and dorsal is top. LN$_v$, sLN$_v$, and lLN$_v$ cell bodies; white arrowhead, sLN$_v$ dorsal projection. All images are representative of 10 or more brain hemispheres.

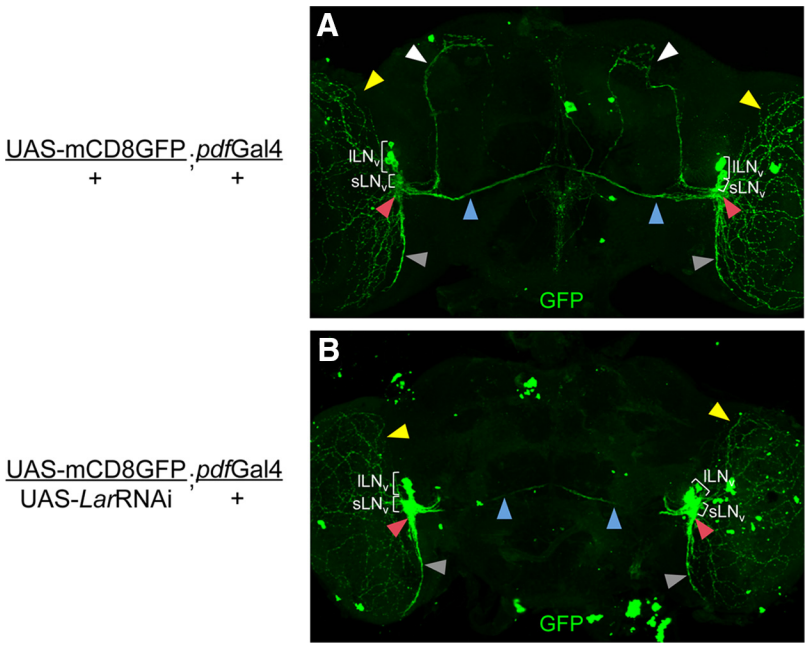

Figure 6. PDF neuron-specific *Lar* RNAi knockdown eliminates the sLN_v dorsal projection. Brains were dissected from adult flies collected at ZT2, immunostained with GFP antibody, and imaged by confocal microscopy. Projected *Z*-series images of whole brains are shown, where lateral is left and dorsal is at the top. ***A***, Seventy-six micrometer projected *Z*-series image from a control UAS-mCD8GFP/+;*pdf*Gal4/+ fly brain. ***B***, Seventy-eight micrometer projected *Z*-series image from a UAS-mCD8GFP/UAS-*Lar*-RNAi;*pdf*Gal4/+ fly brain. White arrowhead, sLN_v dorsal projection; blue arrowhead, lLN_v POT projection; yellow arrowhead, lLN_v medulla projection; red arrowhead, sLN_v and lLN_v aMe projections; gray arrowhead, lLN_v aMe ventral elongation projection. All images are representative of 12 or more brain hemispheres.

Given that the expression of *Lar* RNAi in PDF neurons after eclosion does not alter rhythmic activity, we expected PDF to accumulate in sLN_v dorsal projections. Indeed, we observed PDF staining in sLN_v cell bodies and dorsal projections from flies expressing *Lar* RNAi in PDF neurons after eclosion that was comparable to controls (Fig. 5*A–F*). In contrast, flies that express *Lar* RNAi in PDF neurons during development lacked PDF staining when tested at 18°C as adults (Fig. 5*G–L*). Together, these results demonstrate that *Lar* functions during development to permit PDF accumulation in sLN_v dorsal projections and drive activity rhythms.

Lar disrupts the development of sLN_v dorsal projections

During fly development, LAR was previously shown to regulate neuronal morphology, axon guidance and growth in embryos via multiple signaling pathways (eg, BMP, WNT) (Krueger et al., 1996; Desai et al., 1997; Wills et al., 1999; Kaufmann et al., 2002; Berke et al., 2013). Given that *Lar* plays a role in axonal development, we tested whether sLN_v dorsal projections were disrupted in PDF neuron-specific *Lar* RNAi knockdown flies. sLN_v axonal morphology was visualized with a membrane-tethered version of GFP (mCD8-GFP) expressed in PDF-positive neurons. GFP was detected in sLN_v dorsal projections from control brains at ZT2 (Fig. 6*A*), when the axonal arbor is at its maximum (Fernández et al., 2008). Strikingly, sLN_v dorsal projections were either completely absent (17 of 18 brain hemispheres) or weakly detected (1 of 18 brain hemispheres) in UAS-*Lar*RNAi/UAS-mCD8GFP;*pdf*-Gal4/+ adults beyond the dorsomedial defasciculation point (Fig. 6*B*). Likewise, lLN_v projections to the medulla and the POT were aberrant (8 of 18 brain hemispheres with absent or altered projections) and GFP staining was weak in UAS-*Lar*RNAi/UAS-mCD8GFP;*pdf*Gal4/+ flies (Fig. 6*B*). These results show that *Lar* plays a critical role in the development of sLN_v dorsal projections (and to a lesser extent in lLN_v projections), consistent with the loss of PDF accumulation in these processes and loss of behavioral rhythms.

Although *Lar* mutants and RNAi knockdowns eliminate PDF expression in sLN_v dorsal projections (Fig. 3), PDF continues to accumulate in sLN_v and lLN_v cell bodies and their projections into the medulla, the aMe, and (to a lesser extent) the POT (Figs. 3, 5, 6). The presence of PDF in sLN_v and lLN_v cell bodies and their remaining projections distinguishes *Lar* mutant and RNAi knockdown flies from the pdf^{01} mutant, which eliminates PDF without altering sLN_v structure, or PDF neuron ablation flies, which eliminate both PDF and LN_vs (Renn et al., 1999). Despite their differences in PDF expression and sLN_v structure, *Lar* mutant and RNAi knockdown, pdf^{01} mutant and LN_v ablation flies all abolish activity rhythms in DD. However, activity rhythms of pdf^{01} mutant and LN_v ablated flies are also disrupted in diurnal (LD) cycles; the evening activity peak is advanced by 0.5–1 h and anticipation of lights-on is abolished (Renn et al., 1999). *Lar* RNAi knockdown flies were therefore tested to determine whether their diurnal activity reflected that of pdf^{01} mutant flies, but surprisingly the phase of their evening activity peak was similar to wild-type controls ($p \geq 0.07$) and significantly later ($p < 0.001$) than the pdf^{01} mutant, and they could anticipate lights-on significantly better ($p < 0.05$) than the pdf^{01} mutant (Fig. 7; Table 4). Because PDF expression in LN_v cell bodies and their projections into the medulla, aMe and POT persist in *Lar* RNAi knockdown flies, PDF secretion from LN_vs could account for the difference in light-driven activity.

Discussion

To identify phosphatases that target clock proteins, we performed a clock-cell-specific RNAi screen. In this screen, we found that RNAi knockdown of the RPTP LAR abolishes locomotor activity rhythms (Table 1; Fig. 1). A transheterozygous combination of *Lar* Df and $Lar^{13.2}$ mutant alleles also displayed arrhythmic activity, thus confirming the RNAi knockdown phenotype. The loss of rhythmicity in clock-cell-specific *Lar* RNAi knockdown flies and *Lar* Df/$Lar^{13.2}$ mutants is not due to a defect in core oscillator function; CLK, PER and TIM phosphorylation and abundance were similar in *tim*Gal4 driven UAS-*Lar*RNAi and control UAS-*Lar*RNAi fly head extracts (Fig. 2*A*). Likewise, PER oscillations in pacemaker neurons from *Lar* RNAi knockdown flies were indistinguishable from controls lacking *Lar* RNAi expression (Fig. 2*B*). The presence of an intact molecular clock in *Lar* Df/$Lar^{13.2}$ mutant and clock-cell-specific RNAi knockdown flies suggests that *Lar* disrupts output from the circadian oscillator.

The loss of activity rhythms in *Lar* mutant and RNAi knockdown flies is reminiscent of the arrhythmicity seen in pdf^{01} flies during constant darkness (Renn et al., 1999). Mutations that eliminate PDF (or the PDF receptor) are thought to disrupt output signaling from the sLN_vs to other tissues and synchronizing cues to different groups of pacemaker neurons, thereby causing arrhythmicity in constant darkness (Renn et al., 1999; Peng et al.,

2003; Lin et al., 2004; Hyun et al., 2005; Lear et al., 2005; Mertens et al., 2005). Given these roles for PDF, we hypothesized that loss of *Lar* disrupts PDF expression or release. Indeed, PDF neuron-specific *Lar* RNAi knockdown and *Lar* Df/*Lar*$^{13.2}$ mutants displayed defective PDF staining in sLN$_v$ dorsal projections, but PDF staining persisted in LN$_v$ cell bodies and their remaining projections (Figs. 3, 4). These results suggest that the arrhythmic activity seen in PDF neuron-specific *Lar* RNAi knockdown flies was due to the absence of PDF expression in sLN$_v$ dorsal projections. Expressing *Lar* in clock neurons from *Lar* Df/*Lar*$^{13.2}$ mutants rescued PDF expression in sLN$_v$ dorsal projections and behavioral rhythms (Table 2; Fig. 3*P–R*), demonstrating that *Lar* acts in clock cells to mediate PDF release and/or accumulation in sLN$_v$ dorsal projections and drive rhythmic activity.

PDF expression in sLN$_v$ dorsal projections is first detected in L1 larval brains (Helfrich-Förster, 1997). Since *Lar* participates in axon guidance through the midline during development of the embryonic CNS (Seeger et al., 1993), positioning sensory terminals in the olfactory lobe (Jhaveri et al., 2004), and proper compartmentalization of the visual system (Tayler et al., 2004), *Lar* could function during development, in adults, or both to promote PDF accumulation in sLN$_v$ dorsal projections. Using the Gal80^{ts} TARGET system to express PDF neuron-specific *Lar* RNAi during development, in adults, or both, we found that *Lar* acts during development to enable PDF accumulation in sLN$_v$ dorsal projections (Table 3; Fig. 5). Because PDF functions to synchronize pacemaker neurons and drive behavioral outputs (Park et al., 2000; Peng et al., 2003; Lin et al., 2004; Collins et al., 2012; Cavanaugh et al., 2014), loss of PDF in sLN$_v$ dorsal projections likely accounts for the lack of activity rhythms.

Given that *Lar* is involved in axonal development, *Lar* could also be required for sLN$_v$ dorsal projection development rather than PDF accumulation *per se*. Indeed, sLN$_v$ dorsal processes marked by mCD8-GFP were severely disrupted or absent in PDF neuron-specific *Lar* RNAi knockdown flies (Fig. 6*B*). The lack of sLN$_v$ dorsal projections in PDF neuron-specific *Lar* RNAi knockdown flies implies that *Lar* functions when sLN$_v$ dorsal projections are forming during or before the L1 larval stage (Helfrich-Förster, 1997). Our results suggest that loss of *Lar* alters sLN$_v$ axonal targeting in the dorsal protocerebrum during embryonic or early larval development, thereby impairing PDF signaling, synchronization of the circadian network, and rhythmic activity.

By eliminating sLN$_v$ dorsal projections, *Lar* mutants and RNAi knockdowns disrupt PDF signaling in a novel fashion; *pdf*^{01} flies have intact sLN$_v$s but lack PDF expression and PDF neuron ablated flies eliminate sLN$_v$s entirely and lack PDF expression (Renn et al., 1999). In addition to their arrhythmic activity in DD, *pdf*^{01} mutants and PDF neuron ablated flies lack morning activity in anticipation of lights-on and display an evening peak in activity ~0.5–1 h earlier than wild-type flies in LD, suggesting that the loss of PDF accounts for both of these diurnal phenotypes (Renn et al., 1999). Unexpectedly, *Lar* RNAi knockdown flies were active in anticipation of lights-on and showed an evening activity peak having a wild-type phase in LD cycles (Fig. 7; Table 4). Although PDF signaling to the dorsal brain is disrupted in *Lar* mutants and RNAi knockdowns, PDF continues to be expressed in sLN$_v$ and lLN$_v$ cell bodies and projections that target the medulla, POT and aMe (Figs. 3, 5, 6). These results imply that PDF signaling from the remaining sLN$_v$ and lLN$_v$ projections mediates normal diurnal activity with a morning (M) peak at dawn and an evening (E) peak at dusk.

In *Drosophila*, sLN$_v$s control the M activity peak and LN$_d$s plus the PDF-negative fifth sLN$_v$ control the E activity peak (for review, see Helfrich-Förster, 2014; Beckwith and Ceriani, 2015). Projections from the M (sLN$_v$) neurons and a subset of E (3 LN$_d$ plus fifth sLN$_v$)

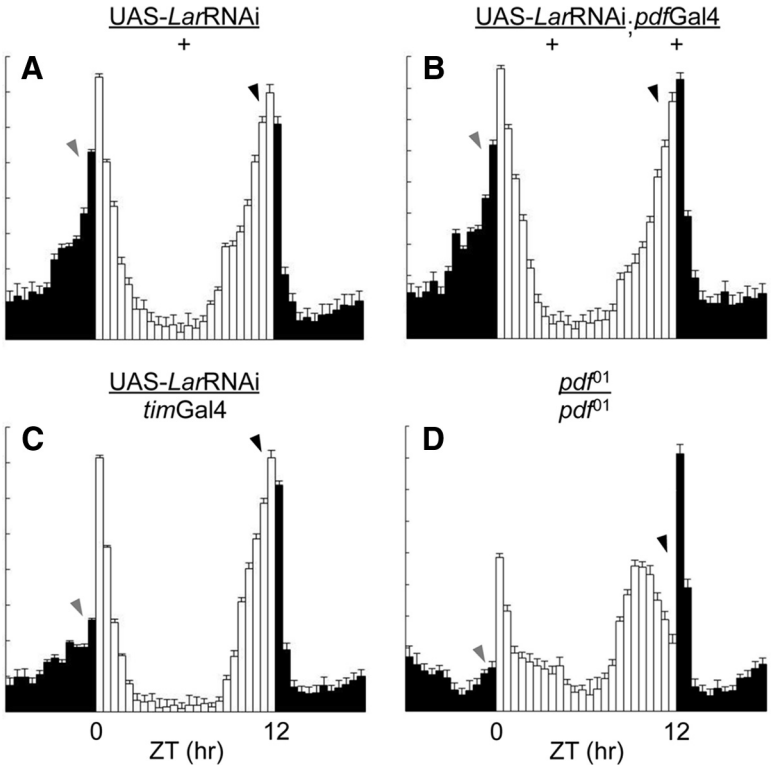

Figure 7. Activity profiles of clock-cell-specific *Lar* RNAi knockdown, *pdf*^{01} and control flies during LD cycles. Average activity histograms indicating relative levels of locomotion for adult males of the indicated genotypes during LD days 2–7 are shown. ***A***, UAS-*Lar*RNAi/+ flies ($n = 16$). ***B***, UAS-*Lar*RNAi/+;*pdf*Gal4/+ flies ($n = 14$). ***C***, UAS-*Lar*RNAi/+;*tim*Gal4/+ flies ($n = 16$). ***D***, *pdf*^{01} mutant flies ($n = 14$). ZT time in hours during an LD cycle where lights-on is ZT0 and lights-off is ZT12; white bars, daytime activity; black bars, night time activity; lights-on anticipation, gray arrow; lights-off anticipation, black arrow.

Table 4. LD activity in clock-cell-specific *Lar* RNAi knockdown flies does not display defects seen in *pdf*^{01} mutants

Genotype	Total	Evening peak ± SEM	Morning peak ± SEM	Anticipation index ± SEM
w^{1118};UAS-*Lar*RNAi/+;+	16	12.0 ± 0.08	0.6 ± 0.08	0.79 ± 0.04
w^{1118};UAS-*Lar*RNAi/*tim*Gal4;+	16	12.1 ± 0.06†	0.5 ± 0.00	0.95 ± 0.03^
w^{1118};UAS-*Lar*RNAi/+;*pdf*Gal4/+	14	12.3 ± 0.07†	0.5 ± 0.04	0.82 ± 0.06‡
y w;+;*pdf*^{01}/*pdf*^{01}	14	9.8 ± 0.03*	0.6 ± 0.08	0.60 ± 0.06$^{\#}$

Adult males were analyzed for behavioral rhythms during LD for at least 7 d. The phase of activity peaks and the anticipation of lights-on during LD cycles were analyzed as described (see Materials and Methods). Total, number of flies analyzed; Morning peak ± SEM, Zeitgeber Time of the morning activity peak ± SEM; Evening peak ± SEM, Zeitgeber Time of the evening activity peak ± SEM; Anticipation index ± SEM, the amount of activity that occurs in anticipation of lights-on ± SEM.

*Significantly different ($p < 0.001$) compared to clock-cell-specific *Lar* RNAi knockdown and control strains.

$^{\#}$Significantly different ($p < 0.05$) compared to clock-cell-specific *Lar* RNAi knockdown and control strains.

†Not different ($p \geq 0.07$) than *w*^{1118};UAS-*Lar*RNAi/+;+ control.

‡Not different ($p = 0.73$) than *w*^{1118};UAS-*Lar*RNAi/+;+ control.

^Significantly better anticipation ($p = 0.02$) than *w*^{1118};UAS-*Lar*RNAi/+;+ control.

neurons, together with those from lLN_vs, terminate in the aMe (Helfrich-Förster et al., 2007; Helfrich-Förster, 2014), a structure that is well preserved in *Lar* mutants and RNAi knockdowns. Importantly, the lLN_vs play a major role in conveying light input from multiple cellular sources (eg, retinal photoreceptors, Hofbauer-Buchner eyelets, and lLN_vs) to the circadian system (Helfrich-Förster et al., 2002, 2007; Shang et al., 2008; Sheeba et al., 2008; Fogle et al., 2011). PDF signaling by lLN_vs is known to phase advance (shorten the period) of M neurons and phase delay (lengthen the period) of E neurons (Wülbeck et al., 2008; Helfrich-Förster, 2014), suggesting that lLN_vs communicate with M and E neurons to define the pattern of diurnal activity. Consistent with this possibility, the M and E neurons that project into the aMe express the PDF receptor (PDFR; Im et al., 2011; Helfrich-Förster, 2014), and are thus capable of responding to PDF. Our results, together with those from previous studies, suggest a model for how diurnal rhythms are regulated; lLN_vs receive light input, release PDF into the aMe, PDFR receptive E cells and M cells are phase delayed and phase advanced, respectively, thereby positioning the E activity peak at the lights-off transition and the M activity peak at the lights-on transition. Signaling by other neuropeptides and neurotransmitters may also be involved in mediating normal peaks of M and E activity in *Lar* mutant and RNAi knockdown flies (for review, see Beckwith and Ceriani, 2015), but additional studies will be necessary to define the relevant signaling pathways and targets. Because the aMe houses the circadian pacemaker center in many insects (Homberg et al., 1991; Stengl and Homberg, 1994; Frisch et al., 1996; Helfrich-Förster et al., 1998; Helfrich-Förster, 2005), it may play a conserved role in regulating diurnal activity rhythms.

LAR presumably functions to dephosphorylate substrates in sLN_vs that enable proper growth and targeting of dorsal projections. Previous work shows that *Lar* is required for segmental nerve b motoneuron growth cones to recognize and enter their correct target regions, suggesting that LAR regulates the phosphorylation state of intracellular target proteins critical for growth cone guidance (Krueger et al., 1996; Wills et al., 1999). It is likely that a dynamic balance of kinase and phosphatase activities at the leading edge of the growth cone endows it with the ability to integrate convergent signals and translate them into appropriate steering decisions. This suggests that *Lar* is a necessary component in a ligand-mediated mechanism that normally guides axons through their appropriate choice points during the development of sLN_v axon architecture in the fly brain. Several LAR extracellular ligands, such as syndecan, dally like protein, and laminin-nidogen complex have been identified that contribute to motor axon guidance and synaptogenesis in flies and/or mammals (O'Grady et al., 1998; Fox and Zinn, 2005; Johnson et al., 2006). Intracellular substrates of LAR include β-catenin and p130cas, which control neurite outgrowth and apoptosis, respectively, depending on their phosphorylation state (Kypta et al., 1996; Weng et al., 1999; Xu and Fisher, 2012). Whether any of these LAR ligands or substrates contribute to sLN_v dorsal projection development will require further investigation. Given that the PTP-containing intracellular domain of *Drosophila* LAR is 77% identical to its human ortholog (Streuli et al., 1989), it is possible that human *Lar* also plays a role in the development of pacemaker neuron processes in the suprachiasmatic nucleus.

References

Akten B, Jauch E, Genova GK, Kim EY, Edery I, Raabe T, Jackson FR (2003) A role for CK2 in the *Drosophila* circadian oscillator. Nat Neurosci 6:251–257. CrossRef Medline

Akten B, Tangredi MM, Jauch E, Roberts MA, Ng F, Raabe T, Jackson FR (2009) Ribosomal s6 kinase cooperates with casein kinase 2 to modulate the *Drosophila* circadian molecular oscillator. J Neurosci 29:466–475. CrossRef Medline

Andreazza S, Bouleau S, Martin B, Lamouroux A, Ponien P, Papin C, Chélot E, Jacquet E, Rouyer F (2015) Daytime CLOCK dephosphorylation is controlled by STRIPAK complexes in *Drosophila*. Cell Rep 11:1266–1279. CrossRef Medline

Beckwith EJ, Ceriani MF (2015) Communication between circadian clusters: the key to a plastic network. FEBS Lett 589:3336–3342. CrossRef Medline

Berke B, Wittnam J, McNeill E, Van Vactor DL, Keshishian H (2013) Retrograde BMP signaling at the synapse: a permissive signal for synapse maturation and activity-dependent plasticity. J Neurosci 33:17937–17950. CrossRef Medline

Cavanaugh DJ, Geratowski JD, Wooltorton JR, Spaethling JM, Hector CE, Zheng X, Johnson EC, Eberwine JH, Sehgal A (2014) Identification of a circadian output circuit for rest:activity rhythms in *Drosophila*. Cell 157:689–701. CrossRef Medline

Chiu JC, Ko HW, Edery I (2011) NEMO/NLK phosphorylates PERIOD to initiate a time-delay phosphorylation circuit that sets circadian clock speed. Cell 145:357–370. CrossRef Medline

Collins B, Kane EA, Reeves DC, Akabas MH, Blau J (2012) Balance of activity between LN(v)s and glutamatergic dorsal clock neurons promotes robust circadian rhythms in *Drosophila*. Neuron 74:706–718. CrossRef Medline

De J, Varma V, Saha S, Sheeba V, Sharma VK (2013) Significance of activity peaks in fruit flies, *Drosophila* melanogaster, under seminatural conditions. Proc Natl Acad Sci U S A 110:8984–8989. CrossRef Medline

Desai CJ, Krueger NX, Saito H, Zinn K (1997) Competition and cooperation among receptor tyrosine phosphatases control motoneuron growth cone guidance in *Drosophila*. Development 124:1941–1952. Medline

Dietzl G, Chen D, Schnorrer F, Su KC, Barinova Y, Fellner M, Gasser B, Kinsey K, Oppel S, Scheiblauer S, Couto A, Marra V, Keleman K, Dickson BJ (2007) A genome-wide transgenic RNAi library for conditional gene inactivation in *Drosophila*. Nature 448:151–156. CrossRef Medline

Fang Y, Sathyanarayanan S, Sehgal A (2007) Post-translational regulation of the *Drosophila* circadian clock requires protein phosphatase 1 (PP1). Genes Dev 21:1506–1518. CrossRef Medline

Fernández MP, Berni J, Ceriani MF (2008) Circadian remodeling of neuronal circuits involved in rhythmic behavior. PLoS Biol 6:e69. CrossRef Medline

Fogle KJ, Parson KG, Dahm NA, Holmes TC (2011) CRYPTOCHROME is a blue-light sensor that regulates neuronal firing rate. Science 331:1409–1413. CrossRef Medline

Fox AN, Zinn K (2005) The heparan sulfate proteoglycan syndecan is an *in vivo* ligand for the *Drosophila* LAR receptor tyrosine phosphatase. Curr Biol 15:1701–1711. CrossRef Medline

Frisch B, Fleissner G, Brandes C, Hall JC (1996) Staining in the brain of *Pachymorpha sexguttata* mediated by an antibody against a *Drosophila* clock-gene product: labeling of cells with possible importance for the beetle's circadian rhythms. Cell Tissue Res 286:411–429. CrossRef Medline

Glossop NR, Hardin PE (2002) Central and peripheral circadian oscillator mechanisms in flies and mammals. J Cell Sci 115:3369–3377. Medline

Hardin PE (2011) Molecular genetic analysis of circadian timekeeping in *Drosophila*. Adv Genet 74:141–173. CrossRef Medline

Hardin PE, Panda S (2013) Circadian timekeeping and output mechanisms in animals. Curr Opin Neurobiol 23:724–731. CrossRef Medline

Harrisingh MC, Wu Y, Lnenicka GA, Nitabach MN (2007) Intracellular Ca2+ regulates free-running circadian clock oscillation *in vivo*. J Neurosci 27:12489–12499. CrossRef Medline

Helfrich-Förster C (1997) Development of pigment-dispersing hormone-immunoreactive neurons in the nervous system of *Drosophila melanogaster*. J Comp Neurol 380:335–354. CrossRef Medline

Helfrich-Förster C (2003) The neuroarchitecture of the circadian clock in the brain of *Drosophila melanogaster*. Microsc Res Tech 62:94–102. CrossRef Medline

Helfrich-Förster C (2005) Organization of endogenous clocks in insects. Biochem Soc Trans 33:957–961. CrossRef Medline

Helfrich-Förster C (2014) From neurogenetic studies in the fly brain to a concept in circadian biology. J Neurogenet 28:329–347. CrossRef Medline

Helfrich-Förster C, Stengl M, Homberg U (1998) Organization of the circadian system in insects. Chronobiol Int 15:567–594. CrossRef Medline

Helfrich-Förster C, Edwards T, Yasuyama K, Wisotzki B, Schneuwly S, Stanewsky R, Meinertzhagen IA, Hofbauer A (2002) The extraretinal

eyelet of *Drosophila*: development, ultrastructure, and putative circadian function. J Neurosci 22:9255–9266. Medline

Helfrich-Förster C, Shafer OT, Wülbeck C, Grieshaber E, Rieger D, Taghert P (2007) Development and morphology of the clock-gene-expressing lateral neurons of *Drosophila melanogaster*. J Comp Neurol 500:47–70. CrossRef Medline

Homberg U, Wurden S, Dircksen H, Rao KR (1991) Comparative anatomy of pigment-dispersing hormon- immunoreactive neurons in the brain of orthopteriod insects. Cell Tissue Res 266:343–357. CrossRef

Houl JH, Ng F, Taylor P, Hardin PE (2008) CLOCK expression identifies developing circadian oscillator neurons in the brains of *Drosophila* embryos. BMC Neurosci 9:119. CrossRef Medline

Hyun S, Lee Y, Hong ST, Bang S, Paik D, Kang J, Shin J, Lee J, Jeon K, Hwang S, Bae E, Kim J (2005) *Drosophila* GPCR Han is a receptor for the circadian clock neuropeptide PDF. Neuron 48:267–278. CrossRef Medline

Im SH, Li W, Taghert PH (2011) PDFR and CRY signaling converge in a subset of clock neurons to modulate the amplitude and phase of circadian behavior in *Drosophila*. PLoS One 6:e18974. CrossRef Medline

Jhaveri D, Saharan S, Sen A, Rodrigues V (2004) Positioning sensory terminals in the olfactory lobe of *Drosophila* by Robo signaling. Development 131:1903–1912. CrossRef Medline

Johnson KG, Tenney AP, Ghose A, Duckworth AM, Higashi ME, Parfitt K, Marcu O, Heslip TR, Marsh JL, Schwarz TL, Flanagan JG, Van Vactor D (2006) The HSPGs Syndecan and Dallylike bind the receptor phosphatase LAR and exert distinct effects on synaptic development. Neuron 49:517–531. CrossRef Medline

Kaufmann N, DeProto J, Ranjan R, Wan H, Van Vactor D (2002) *Drosophila* liprin-alpha and the receptor phosphatase Dlar control synapse morphogenesis. Neuron 34:27–38. CrossRef Medline

Kloss B, Price JL, Saez L, Blau J, Rothenfluh A, Wesley CS, Young MW (1998) The *Drosophila* clock gene *double-time* encodes a protein closely related to human casein kinase Iε. Cell 94:97–107. CrossRef Medline

Kloss B, Rothenfluh A, Young MW, Saez L (2001) Phosphorylation of *period* is influenced by cycling physical associations of *double-time*, period, and timeless in the *Drosophila* clock. Neuron 30:699–706. CrossRef Medline

Krueger NX, Van Vactor D, Wan HI, Gelbart WM, Goodman CS, Saito H (1996) The transmembrane tyrosine phosphatase DLAR controls motor axon guidance in *Drosophila*. Cell 84:611–622. CrossRef Medline

Kypta RM, Su H, Reichardt LF (1996) Association between a transmembrane protein tyrosine phosphatase and the cadherin-catenin complex. J Cell Biol 134:1519–1529. CrossRef Medline

Lear BC, Merrill CE, Lin JM, Schroeder A, Zhang L, Allada R (2005) A G protein-coupled receptor, groom-of-PDF, is required for PDF neuron action in circadian behavior. Neuron 48:221–227. CrossRef Medline

Lin JM, Kilman VL, Keegan K, Paddock B, Emery-Le M, Rosbash M, Allada R (2002) A role for casein kinase 2alpha in the *Drosophila* circadian clock. Nature 420:816–820. CrossRef Medline

Lin Y, Stormo GD, Taghert PH (2004) The neuropeptide pigment-dispersing factor coordinates pacemaker interactions in the *Drosophila* circadian system. J Neurosci 24:7951–7957. CrossRef Medline

Liu T, Mahesh G, Houl JH, Hardin PE (2015) Circadian activators are expressed days before they initiate clock function in late pacemaker neurons from *Drosophila*. J Neurosci 35:8662–8671. CrossRef Medline

Martinek S, Inonog S, Manoukian AS, Young MW (2001) A role for the segment polarity gene *shaggy*/GSK-3 in the *Drosophila* circadian clock. Cell 105:769–779. CrossRef Medline

McGuire SE, Le PT, Osborn AJ, Matsumoto K, Davis RL (2003) Spatiotemporal rescue of memory dysfunction in *Drosophila*. Science 302:1765–1768. CrossRef Medline

Menet JS, Hardin PE (2014) Circadian clocks: the tissue is the issue. Curr Biol 24:R25–R27. CrossRef Medline

Mertens I, Vandingenen A, Johnson EC, Shafer OT, Li W, Trigg JS, De Loof A, Schoofs L, Taghert PH (2005) PDF receptor signaling in *Drosophila* contributes to both circadian and geotactic behaviors. Neuron 48:213–219. CrossRef Medline

Nitabach MN, Taghert PH (2008) Organization of the *Drosophila* circadian control circuit. Curr Biol 18:R84–R93. CrossRef Medline

O'Grady P, Thai TC, Saito H (1998) The laminin-nidogen complex is a ligand for a specific splice isoform of the transmembrane protein tyrosine phosphatase LAR. J Cell Biol 141:1675–1684. CrossRef Medline

Park JH, Helfrich-Förster C, Lee G, Liu L, Rosbash M, Hall JC (2000) Differential regulation of circadian pacemaker output by separate clock genes in *Drosophila*. Proc Natl Acad Sci U S A 97:3608–3613. CrossRef Medline

Partch CL, Green CB, Takahashi JS (2014) Molecular architecture of the mammalian circadian clock. Trends Cell Biol 24:90–99. CrossRef Medline

Peng Y, Stoleru D, Levine JD, Hall JC, Rosbash M (2003) *Drosophila* free-running rhythms require intercellular communication. PLoS Biol 1:E13. CrossRef Medline

Peschel N, Helfrich-Förster C (2011) Setting the clock–by nature: circadian rhythm in the fruitfly *Drosophila melanogaster*. FEBS Lett 585:1435–1442. CrossRef Medline

Pfeiffenberger C, Lear BC, Keegan KP, Allada R (2010) Sleep and circadian behavior monitoring in *Drosophila*. In: *Drosophila* neurobiology: a laboratory manual (Zhang B, Freeman MR, Waddell S, eds), pp 483–504. New York: Cold Spring Harbor.

Price JL, Blau J, Rothenfluh A, Abodeely M, Kloss B, Young MW (1998) double-time is a novel *Drosophila* clock gene that regulates PERIOD protein accumulation. Cell 94:83–95. CrossRef Medline

Renn SC, Park JH, Rosbash M, Hall JC, Taghert PH (1999) A *pdf* neuropeptide gene mutation and ablation of PDF neurons each cause severe abnormalities of behavioral circadian rhythms in *Drosophila*. Cell 99:791–802. CrossRef Medline

Sathyanarayanan S, Zheng X, Xiao R, Sehgal A (2004) Posttranslational regulation of *Drosophila* PERIOD protein by protein phosphatase 2A. Cell 116:603–615. CrossRef Medline

Seeger M, Tear G, Ferres-Marco D, Goodman CS (1993) Mutations affecting growth cone guidance in *Drosophila*: genes necessary for guidance toward or away from the midline. Neuron 10:409–426. CrossRef Medline

Shafer OT, Yao Z (2014) Pigment-dispersing factor signaling and circadian rhythms in insect locomotor activity. Curr Opin Insect Sci 1:73–80. CrossRef Medline

Shang Y, Griffith LC, Rosbash M (2008) Light-arousal and circadian photoreception circuits intersect at the large PDF cells of the *Drosophila* brain. Proc Natl Acad Sci U S A 105:19587–19594. CrossRef Medline

Sheeba V, Fogle KJ, Kaneko M, Rashid S, Chou YT, Sharma VK, Holmes TC (2008) Large ventral lateral neurons modulate arousal and sleep in *Drosophila*. Curr Biol 18:1537–1545. CrossRef Medline

Stengl M, Homberg U (1994) Pigment-dispersing hormone-immunoreactive neurons in the cockroach *Leucophaea maderae* share properties with circadian pacemaker neurons. J Comp Physiol A 175:203–213. CrossRef Medline

Streuli M, Krueger NX, Tsai AY, Saito H (1989) A family of receptor-linked protein tyrosine phosphatases in humans and *Drosophila*. Proc Natl Acad Sci U S A 86:8698–8702. CrossRef Medline

Szabó A, Papin C, Zorn D, Ponien P, Weber F, Raabe T, Rouyer F (2013) The CK2 kinase stabilizes CLOCK and represses its activity in the *Drosophila* circadian oscillator. PLoS Biol 11:e1001645. CrossRef Medline

Tayler TD, Robichaux MB, Garrity PA (2004) Compartmentalization of visual centers in the *Drosophila* brain requires slit and Robo proteins. Development 131:5935–5945. CrossRef Medline

Weng LP, Wang X, Yu Q (1999) Transmembrane tyrosine phosphatase LAR induces apoptosis by dephosphorylating and destabilizing p130Cas. Genes Cells 4:185–196. CrossRef Medline

Wills Z, Bateman J, Korey CA, Comer A, Van Vactor D (1999) The tyrosine kinase Abl and its substrate enabled collaborate with the receptor phosphatase Dlar to control motor axon guidance. Neuron 22:301–312. CrossRef Medline

Wülbeck C, Grieshaber E, Helfrich-Förster C (2008) Pigment-dispersing factor (PDF) has different effects on *Drosophila's* circadian clocks in the accessory medulla and in the dorsal brain. J Biol Rhythms 23:409–424. CrossRef Medline

Xu Y, Fisher GJ (2012) Receptor type protein tyrosine phosphatases (RPTPs): roles in signal transduction and human disease. J Cell Commun Signal 6:125–138. CrossRef Medline

Yoshii T, Rieger D, Helfrich-Förster C (2012) Two clocks in the brain: an update of the morning and evening oscillator model in *Drosophila*. Prog Brain Res 199:59–82. CrossRef Medline

Yu W, Zheng H, Houl JH, Dauwalder B, Hardin PE (2006) PER-dependent rhythms in CLK phosphorylation and E-box binding regulate circadian transcription. Gene Dev 20:723–733. CrossRef Medline

Yu W, Houl JH, Hardin PE (2011) NEMO kinase contributes to core period determination by slowing the pace of the *Drosophila* circadian oscillator. Curr Biol 21:756–761. CrossRef Medline